Agilent Technologies
Innovating the HP Way

Designing the Virtual Battery

Application Note 1088

Abstract

Many of today's portable RF products, such as RF/ID tags used in automotive electronic toll tag applications, are too small to contain a battery sufficient to power them over their expected lifetime. Where such devices operate in the presence of a RF field, a simple and inexpensive circuit consisting of an antenna, one or more Schottky diodes, and a few passive components can be designed to convert part of the illuminating RF field into DC power. This paper will present design techniques and illustrate them with data obtained on prototype circuits.

Introduction

The term "virtual battery" [1] has been coined to describe a simple, compact and low cost replacement for a battery in RF tags and other portable applications were three design considerations apply:

1. The RF application to be powered is very small and portable.

2. The design lifetime of the application is long.

3. The application does not require primary power in the absence of an illuminating RF field.

A good example of such an application is the modulated backscatter type of RF/ID tag [2], which operates only when passing through a highway toll booth and which is expected to last five years or more without service. The interrogator in the toll booth includes a 915 MHz transmitter which illuminates the tag with a relatively robust RF field, providing a source of energy to be converted by the virtual battery. As shown in the section below, such virtual batteries consist of an antenna, one or two Schottky diodes and one or more inexpensive passive components.

Such a circuit is a variation on the ordinary video detector [3],[4]. Design considerations are presented and test data are provided for a practical circuit.

Schottky Detector Circuits

The Schottky diode can be represented by a linear equivalent circuit, as shown in Figure 1.

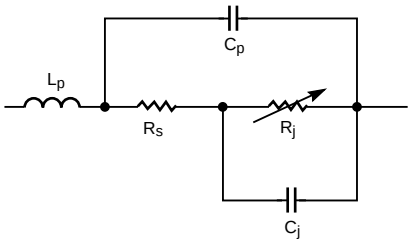

Figure 1. Equivalent Circuit of a Schottky Diode.

C_j is the parasitic junction capacitance of the Schottky chip and R_S is parasitic series resistance of the chip. L_p and C_p are package parasitics. R_j is the junction resistance of the diode, where RF power is converted into DC output voltage. For maximum output, all the incoming RF voltage should ideally appear across R_j, with nothing lost in R_S. The equation for junction resistance is:

$$R_j = 0.026 / I_T \qquad (1)$$

where

I_T = $I_s + I_b + I_o$, in amperes

I_s = the diode's saturation current, a function of Schottky barrier height

I_b = circulating current generated by the rectification of RF power

I_o = External bias current (if any)

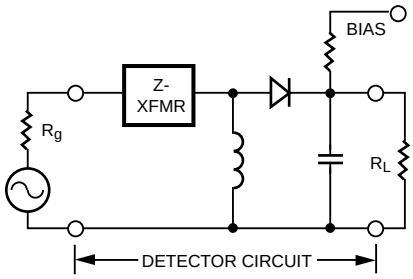

Figure 2: Schottky Detector Circuit.

Such a diode can be used to convert RF power to DC with a simple detector circuit, as shown in Figure 2.

The behavior of Schottky detector circuits has been well studied in an operating region defined by two conditions: low input power (square law operation) and high load resistance. These two conditions, however, are not consistent with the use of a Schottky diode to generate reasonable levels of DC voltage and current.

A recent analysis [5] provides a single equation which describes the operation of a Schottky diode over the entire practical range of input power and load resistance.

$$I_o\left(\frac{\Lambda}{n}\sqrt{8R_gP_{inc}}\right)=\left(1+\frac{I_o}{I_s}+\frac{V_o}{R_L\,I_s}\right) \cdot \exp\left\{\left[1+\frac{R_g+R_s}{R_L}\right]\frac{\Lambda}{n}\,V_o + \frac{\Lambda}{n}R_S\,I_o\right\} \quad (2)$$

where
I_o = zero order Bessel function
P_{inc} = incident RF power
R_g = generator or source impedance
n = diode ideality factor (emission coefficient)
$\Lambda = q / (kT)$
q = electronic charge
k = Boltzmann's constant
T = temperature in degrees Kelvin
R_L = output load resistance
V_o = output voltage

This equation neglects the effects of diode package parasitics (which can easily be absorbed into the input matching network), junction capacitance C_j , and (therefore) frequency. However, as shall be seen later, these necessary simplifications are quite reasonable in the analysis of virtual batteries operating at RF frequencies. The equation also neglects the effect of RF impedance matching at the input to the diode, a matter which will be treated in a later section.

Equation (2) presents the *input* (P_{inc}) as a function of *output* (V_o), as is often the case when obtaining the solution of a nonlinear problem. To solve (2), it is necessary to obtain the inverse of the Bessel function. Such an equation is easily analyzed by a program such as Mathcad(1), where the output voltage can be iterated to obtain a series of values for P_{inc}, after which a plot of V_o vs. P_{inc} can be made. Appendix A is a printout of the Mathcad file used to obtain the plots shown in this paper.

It should be noted that equation (2) is useful only if accurate values of the diode parameters I_s, n, and R_s are used. These are generally provided by the diode manufacturer, or they can be determined from measurements as described in Appendix B.

Schottky diodes have evolved into many designs, which can be reduced to two basic categories. The first, those formed on n-type silicon, are characterized by relatively high barrier heights and low values of series resistance — these are ideal for mixer applications and detectors where DC bias is available. The second type are formed on p-type silicon, and are distinguished by low barrier height (high I_s) and high R_s. These diodes were developed for square law detector applications where load resistance is high and DC bias is not available. Both types were evaluated for virtual battery applications. Table 1 lists the characteristics of two microwave diodes, both having $C_j \cong 0.25$ pF, which were analyzed and measured.

Table 1. Diode Parameters

	n-type	p-type
Part	HSMS-8201	HSMS-2850
n	1.12	1.17
I_S (A)	55×10^{-9}	2×10^{-6}
R_S (Ω)	7	25

Using equation (2), the calculated transfer curve for these two diodes was obtained as shown in Figure 3.

As can be seen, the higher saturation current of the p-type diode results in a substantially higher output voltage at low power levels where square law detectors typically operate. However, at output voltage levels of interest for this paper, the differences between the two types of diodes appears to disappear.

Two sample diodes, having the characteristics given in Table 1, were mounted on the end of a 50 Ω transmission line with no matching

(1) Product of MathSoft, Inc., 201 Broadway, Cambridge, Massachusetts.

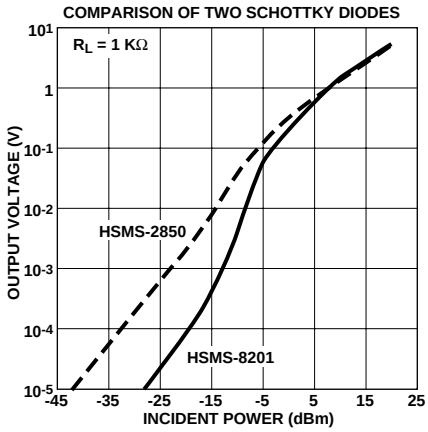

Figure 3. Calculated Transfer Curves.

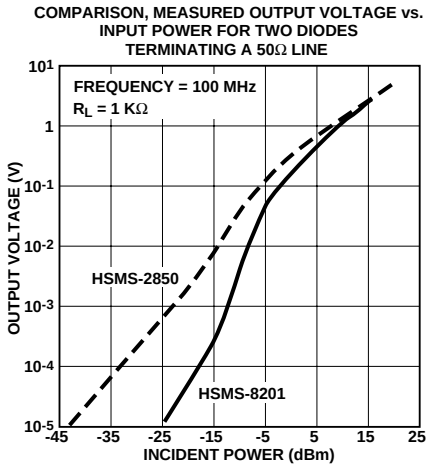

Figure 4. Measured Transfer Curves.

network and transfer curves were measured, as shown in Figure 4.

The agreement between these data and the calculations shown in Figure 3 is very good.

Voltage Doublers

The primary goal of a virtual battery circuit is maximum voltage at a given power level. The voltage doubler [6] provides a higher output than the single diode shown in Figure 2. It is illustrated in Figure 5 (zero bias or virtual battery configuration).

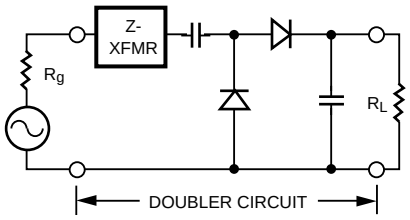

Figure 5. The Voltage Doubler

The doubler puts the Schottky diodes in parallel with respect to the input RF signal, which lowers the input impedance and reduces the difficulty of the impedance matching network. However, the diodes appear in series with respect to the output load, which (approximately) doubles the voltage. If the two diodes are contained in a single SOT-23 package, the cost impact associated with the second diode is very small, making the doubler an interesting circuit for virtual battery applications.

In Figure 6, an equivalent circuit is evolved for the doubler, by means of which it can be analyzed using equation (2).

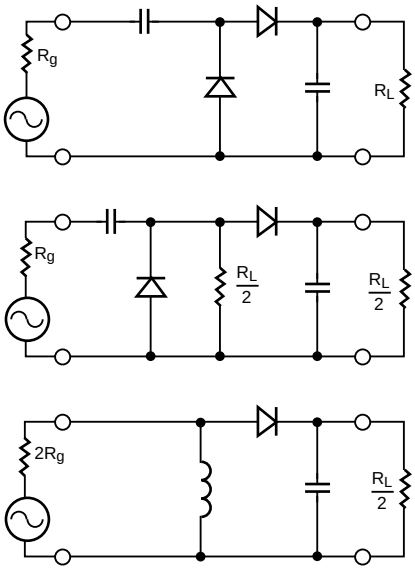

Figure 6. Doubler Equivalent Circuit.

It can be seen that the transfer curve for a doubler can be predicted using equation (2) by doubling the value of R_g, halving the value of R_L and doubling the calculated values of V_o.

Calculations were made for a doubler using the p-type diode described in Table 1, and such a diode pair (the HSMS-2852) was placed on the end of a 50 Ω transmission line with no RF matching network. Both calculated and measured data for this doubler, as well as for the single diode shown in Figures 3 and 4, are given in Figure 7.

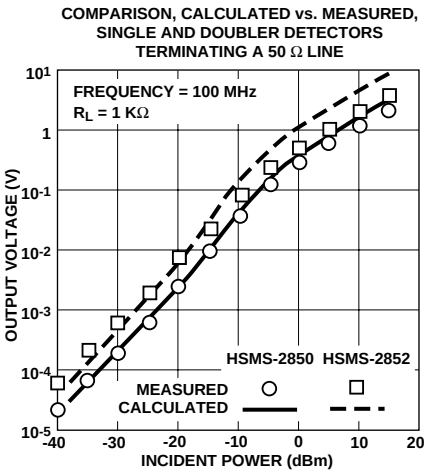

Figure 7. Data for an Unmatched Doubler.

Agreement between calculated and measured data is not as good as it was for the single diode case, but is adequate nonetheless. Both calculated and measured curves predict a substantial improvement in output voltage for the doubler, when compared to a single diode circuit.

Junction Capacitance

The effect of the diode's junction capacitance is to short out the junction resistance, diverting incoming RF energy into the parasitic series resistance where it does no useful work. At high frequencies and high values of R_j, as are typical of square law detectors, junction capacitance has a large effect upon output voltage.

The effect of capacitance on output voltage is given by [7]:

$$M = \frac{1}{1 + \omega^2 C_j^2 R_S R_j} \qquad (3)$$

Where

$\omega = 2\pi$ times frequency

M = a multiplier for V_O

While this equation is an approximation, its accuracy is quite good for our purposes.

If M is plotted against junction resistance, the curve of Figure 8 is the result.

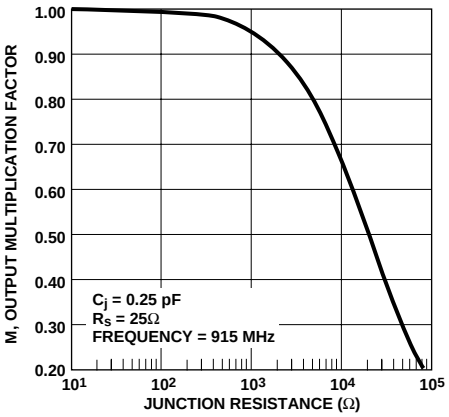

Figure 8. The Effect of C_j .

At the input power levels of interest to this analysis, output voltages will be in excess of 1 V and circulating current I_b will be on the order of 0.1 mA or more. At these levels of current R_j is less than 250 Ω, and junction capacitance has no significant effect.

RF Impedance Matching

When the input impedance of the virtual battery or detector circuit is other than the complex conjugate of the source, some incident RF power is reflected back to the source and lost. In the case of the square law (small signal) detector, R_j is fixed by the diode's saturation current or the circuit's bias current. This value is inserted into the linear equivalent circuit of Figure 1 and a RF matching circuit can be derived. Of course, since $R_j >> 50\ \Omega$, losses in the matching network [4] will reduce the gain in output voltage from a lossless-case value of 50 times to a more realistic value of 10 times.

However, the impedance matching case for the virtual battery is much different. First, the impedance of the diode is much lower owing to the high value of circulating current which depresses R_j. The situation is made even easier when the voltage doubler circuit is used. However, R_j is not a constant for the virtual battery. As input power is increased or load resistance is decreased, the value of circulating current will go up and junction resistance will be reduced. In the virtual battery, R_j is not a constant — it spans a significant range.

As part of the design of a 915 MHz voltage doubler, the impedance of a HSMS-2852 Schottky pair was measured as a function of external bias. The data are shown in Figure 9.

0.3 to 0.5 mA was selected as a probable operating range for the doubler, and the value of R_j was estimated to be 250 Ω for each diode in the pair. The model of Figure 2 was set up for each diode of the pair in a linear analysis program (MMICAD [2]) and a 3-element low pass filter matching section was optimized at the input to the diode pair. The final matching network consisted of a series microstrip transmission line (on 0.032" thick FR4) of length = 1.07" and width = 0.015", with a small capacitive flag at each end. The flags constituted the shunt capaci-

(2) Product of Optotek Limited, 62 Steacie Drive, Kanata, Ontario, Canada K2K 2A9

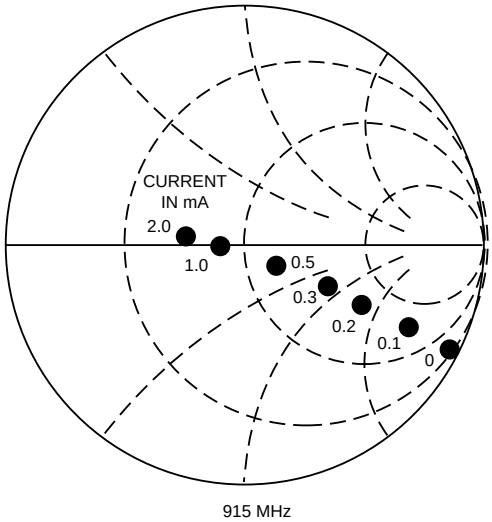

Figure 9. Impedance of a HSMS-2852.

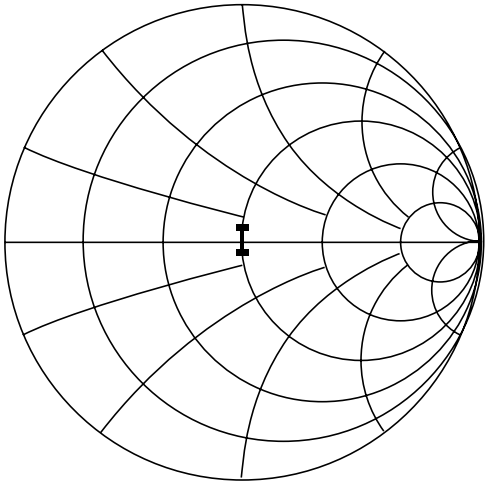

Figure 10. Predicted Input Impedance Match.

tors and the high impedance line the series inductor of the low pass filter. The predicted impedance of this matched diode pair, over the frequency range of 865 to 965 MHz, is shown in Figure 10.

Note that this analysis assumes that the diode is to be matched to a source impedance of 50 + j0, since measurements were to be made using conventional test equipment. In the virtual battery, the antenna is the source, and its impedance is probably something very different from 50 Ω. This may make the design of the actual matching network somewhat more challenging.

Measured Results

The two doubler circuits of the type described above were fabricated on 0.032" thick FR4 microstrip. The first used the HSMS-2852 low barrier diode pair and the second used the HSMS-8202 low R_S diode pair. They were tested, and their performance compared to a small signal (square law) detector created for an earlier work [4]. All three were designed to operate from a source of 50 + j0 Ω at a frequency of 915 MHz.

The two virtual battery circuits were tested for input return loss vs. input power and empirically optimized for minimum VSWR at 0 dBm. In both cases, this optimization resulted in the elimination of the capacitive flags on the input matching network, which was then reduced to a single high impedance (inductive) line. The square law detector, on the other hand, had been designed for optimum match at very small signal levels. Plots of return loss vs. input power for all three circuits are shown in Figure 11.

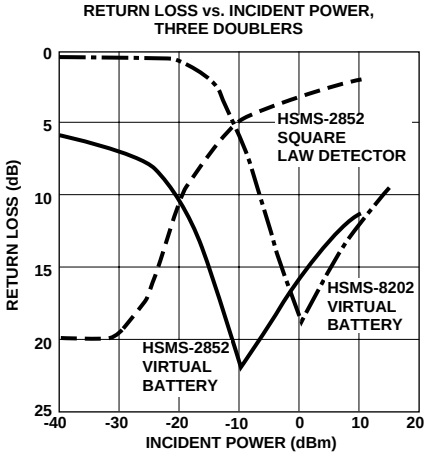

Figure 11. Return Loss vs. Input Power.

All three circuits were characterized for their transfer characteristic with load resistances of 100 KΩ, 1 KΩ and 100 Ω. The curves for R_L = 1 KΩ are shown in Figures 12a and 12b.

It is interesting to note that the square law detector, using the self-biasing low barrier diodes, produces the largest voltage output at very small signal levels. However, at the large signal levels of interest to this analysis, its poor impedance match results in a lower output voltage than the virtual battery which uses the same HSMS-2852 diode pair.

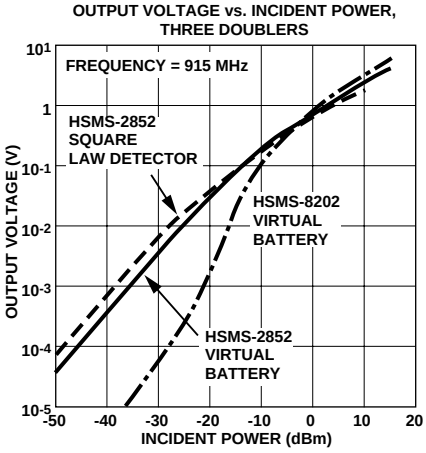

Figure 12a: Transfer Curves for Three Doublers.

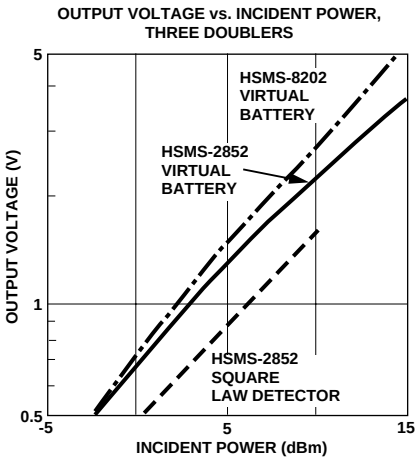

Figure 12b. Transfer Curve, Expanded Scale.

These data lead to a more significant observation. At input power levels below 0 dBm, the HSMS-2852 low barrier pair produces a higher output voltage than the HSMS-8202 low R_s pair. This difference in performance was predicted by equation (2), as illustrated in Figure 3. What was not predicted by equation (2), however, is the significantly higher output voltage produced by the HSMS-8202 at incident power levels greater than 0 dBm. When an impedance matching network is placed before the diode, designed for low values of R_j, the importance of R_s is increased. For example, when the value of total current I_T is increased until $R_j = R_s$, the output voltage of the virtual battery will be half the value it would have been for $R_s = 0$. While this point can be reached at some input power level for any diode type, it is achieved at a much lower value of input power when an impedance matching network is used.

The efficiency (output power/input power) of the two virtual batteries was measured, at an incident power level of +10 dBm, as a function of load resistance. These data are presented in Figure 13.

These data illustrate the significant effect that parasitic series resistance can have on the efficiency of a virtual battery. Peak efficiency was achieved at a load resistance of approximately 2 KΩ, a practical value for virtual battery applications.

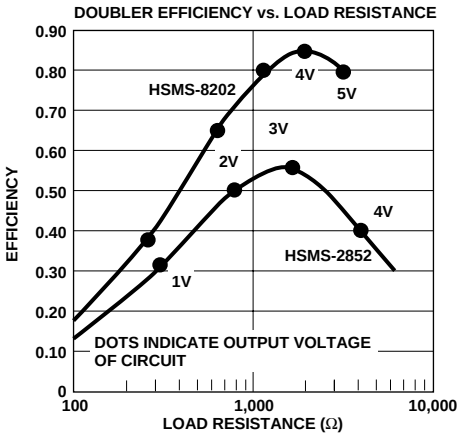

Figure 13. Efficiency vs. Load Resistance.

Conclusion

Design considerations for a virtual battery have been presented, and measured data from practical circuits have been presented. It has been shown that a Schottky diode voltage doubler, with an impedance matching network optimized for high values of incident power, can be an efficient substitute for a larger and more expensive battery in certain applications.

References

[1] Private communication with Robert Myers of Agilent Technologies.

[2] Lawrence Livermore Labs, *An Automatic Vehicle ID System for Toll Collecting,* Lawrence Livermore National Laboratory LLNL Transportation Program, L-644.

[3] Agilent Technologies Application Note 923, *Schottky Barrier Diode Video Detectors.*

[4] Raymond W. Waugh, "Designing Detectors for RF/ID Tags," *Proceedings of RF Expo West,* 1995.

[5] Robert G. Harrison and Xavier Le Polozec, "Nonsquarelaw Behavior of Diode Detectors Analyzed by the Ritz-Galérkin Method," *IEEE Transactions on Microwave Theory and Techniques*, Vol. 42, No. 5, May 1994, pp. 840 - 845.

[6] Agilent Technologies Application Note 956-4, *Schottky Diode Voltage Doubler*.

[7] Agilent Technologies Application Note 969, *The Zero Bias Schottky Detector Diode* (revised 8/94).

Appendix A - Mathcad File

V_O vs. P_{in} calculator, based upon Harrison & Polozec, "Nonsquarelaw Behavior of Diode Detectors Analyzed by the Ritz-Galerkin Method," IEEE Trans MTT, Vol. 42, No. 5, May, 1994. This Mathcad file was developed with the assistance of Bob Gauthier of Mathsoft, Inc.

$t := 25$ in °C

$\Lambda := 38.5 \cdot \frac{300}{275 + t}$

$I_o := 0$ external bias, A

$n := 1.12$ Ideality factor

$I_s := 54 \cdot 10^{-9}$ saturation current, A

$R_g := 50$ Generator impedance, in Ω

$R_S := 7$ in Ω

$R_L := 500$ in Ω

Values shown above are for the HSMS-8201 Schottky diode.

$m := 18, 19 \ldots 43$

$k_m := \frac{m - 40}{4}$

Note that you might have to reduce the high end of this range from 43 to something less for certain sets of input values. If adjustment of guess values z does not result in a solution for $\mathbf{a_{kn}}$, reduce the maximum value of the range for **m**. For small signal analysis, equations A3 through A8 may be deleted.

$V_{om} := 10^{k_m}$ Output voltage is stepped. (A1)

$$B_m := \left(1 + \frac{I_o}{I_s} + \frac{V_{om}}{R_L \cdot I_s}\right) \cdot e^{\left[\left(1 + \frac{R_g + R_S}{R_L}\right) \cdot \frac{\Lambda}{n} \cdot V_{om} + \frac{\Lambda}{n} \cdot R_S \cdot I_o\right]} \quad \text{(A2)}$$

$k1 := 18 \ldots 35 \quad z := 13 \quad a_{k1} := \text{root}\left(\frac{B_{k1}}{B_{k1}} - \frac{IO(z)}{B_{k1}}, z\right)$ (A3)

$k2 := 36 \ldots 39 \quad z := 40 \quad a_{k2} := \text{root}\left(\frac{B_{k2}}{B_{k2}} - \frac{IO(z)}{B_{k2}}, z\right)$ (A4)

$k3 := 40 \quad z := 50 \quad a_{k3} := \text{root}\left(\frac{B_{k3}}{B_{k3}} - \frac{IO(z)}{B_{k3}}, z\right)$ (A5)

$k4 := 41 \quad z := 1.85 \cdot a_{k3} \quad a_{k4} := \text{root}\left(\frac{B_{k4}}{B_{k4}} - \frac{IO(z)}{B_{k4}}, z\right)$ (A6)

$k5 := 42 \quad z := 1.85 \cdot a_{k4} \quad a_{k5} := \text{root}\left(\frac{B_{k5}}{B_{k5}} - \frac{IO(z)}{B_{k5}}, z\right)$ (A7)

$k6 := 43 \quad z := 1.85 \cdot a_{k5} \quad a_{k6} := \text{root}\left(\frac{B_{k6}}{B_{k6}} - \frac{IO(z)}{B_{k6}}, z\right)$ (A8)

$a_{k3} = 52$

$a_{k4} = 82$

$a_{k5} = 136$

$a_{k6} = 231$

$P_{inc_m} := \frac{1}{8 \cdot R_g} \cdot \left(\frac{n \cdot a_m}{\Lambda}\right)^2$ Watts

$dBm_m := 10 \cdot \log\left(P_{inc_m} \cdot 1000\right)$

a_{k2}
14.3
18.0
24.0
34.2

a_{k1}	B_m	V_{om} Volts
0.68	1.117	$3.2 \cdot 10^{-6}$
0.89	1.209	$5.6 \cdot 10^{-6}$
1.17	1.371	$1.0 \cdot 10^{-5}$
1.51	1.660	$1.8 \cdot 10^{-5}$
1.93	2.174	$3.2 \cdot 10^{-5}$
2.42	3.089	$5.6 \cdot 10^{-5}$
2.96	4.722	$1.0 \cdot 10^{-4}$
3.54	7.638	$1.8 \cdot 10^{-4}$
4.15	$1.287 \cdot 10$	$3.2 \cdot 10^{-4}$
4.78	$2.230 \cdot 10$	$5.6 \cdot 10^{-4}$
5.41	$3.952 \cdot 10$	$1.0 \cdot 10^{-3}$
6.07	$7.157 \cdot 10$	$1.8 \cdot 10^{-3}$
6.75	$1.333 \cdot 10^2$	$3.2 \cdot 10^{-3}$
7.47	$2.596 \cdot 10^2$	$5.6 \cdot 10^{-3}$
8.26	$5.446 \cdot 10^2$	$1.0 \cdot 10^{-2}$
9.19	$1.303 \cdot 10^3$	$1.8 \cdot 10^{-2}$
10.35	$3.935 \cdot 10^3$	$3.2 \cdot 10^{-2}$
11.94	$1.795 \cdot 10^4$	$5.6 \cdot 10^{-2}$
	$1.705 \cdot 10^5$	$1.0 \cdot 10^{-1}$
	$5.972 \cdot 10^6$	$1.8 \cdot 10^{-1}$
	$2.127 \cdot 10^9$	$3.2 \cdot 10^{-1}$
	$4.686 \cdot 10^{13}$	$5.6 \cdot 10^{-1}$
	$1.583 \cdot 10^{21}$	1.0
	$2.471 \cdot 10^{34}$	1.8

dBm_m	P_{inc_m} W	a_m
-30.13	$9.71 \cdot 10^{-7}$	$6.8 \cdot 10^{-1}$
-27.74	$1.68 \cdot 10^{-6}$	$8.9 \cdot 10^{-1}$
-25.40	$2.88 \cdot 10^{-6}$	1.2
		1.5

Agilent Technologies
Innovating the HP Way

Appendix B
Diode Parameters

To obtain diode characteristics I_s, n and R_s from laboratory measurements, take the following steps:

1. Measure forward voltage V_1 at I_f = 0.010 mA and V_2 at I_f = 0.100 mA. For most Schottky diodes, these two points fall on that part of the curve which corresponds to an ideal diode characteristic (ie., the effect of R_s is not seen).

2. Measure V_3 and V_4 at I_f = 4.80 mA and 5.20 mA respectively. Note that accurate voltmeters and ammeters, with good resolution, must be used for the measurements in steps 1 and 2.

3. Compute $n = (V_2 - V_1)/0.0586$

4. Compute $I_S = \dfrac{0.010}{e^{(V_1/0.025n)}}$ mA

5. Compute $R_S = \dfrac{V_4 - V_3}{0.0004}$ Ω

5966-0785E (11/99)